

AD-A065 543

MASSACHUSETTS INST OF TECH CAMBRIDGE ARTIFICIAL INTE--ETC F/G 6/2  
THE MINIMUM ENERGY MOVEMENT FOR A SPRING MUSCLE MODEL, (U)  
SEP 77 J M HOLLERBACH

N00014-77-C-0389

UNCLASSIFIED

AI-M-424

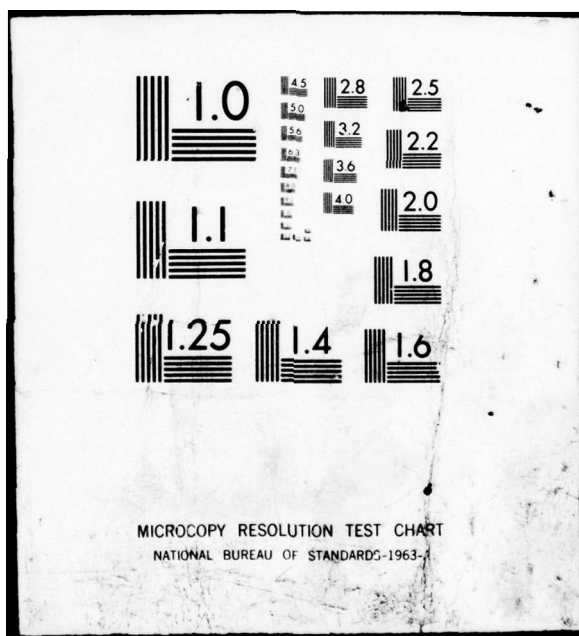
NI

| OF /  
AD 65543



END  
DATE  
FILED

5-79  
DDC



**DDC FILE COPY** **ADA065543**

UNCLASSIFIED

SECURITY CLASSIFICATION OF THIS PAGE (When Data Is Entered)

5

DD FORM 1 JAN 73 1473

EDITION OF 1 NOV 65 IS OBSOLETE  
S/N 0102-014-6601

UNCLASSIFIED

LB

SECURITY CLASSIFICATION OF THIS PAGE (When Data Entered)

20. demonstrated. Some relaxations of the restrictions underlying the spring model  
are shown to preserve the bang-coast-bang solution.

DOC LIFE COPY

MASSACHUSETTS INSTITUTE OF TECHNOLOGY  
ARTIFICIAL INTELLIGENCE LABORATORY

A.I. Memo No. 424

September, 1977

ACCESSION FORM	
BTB	White Section
BDB	Buff Section
ANNOUNCED	
JUSTIFICATION	
BY	
DISTRIBUTION/AVAILABILITY CODES	
DIST.	AVAIL. 800/N SPECIAL
A1	

The Minimum Energy Movement  
for a Spring Muscle Model

John M. Hollerbach

ABSTRACT. There are many ways of programming an actuator or effector for movement between the same two points. In the interest of efficiency it is sometimes desirable to program that trajectory which requires the least amount of energy. This paper considers the minimum energy movement for a spring-like actuator abstracted from muscle mechanics and energetics. It is proved that for this actuator a bang-coast-bang actuation pattern minimizes the energy expenditure. For some parameter values this pattern is modified by a singular arc at the first switching point. A surprising limitation on the duration of coast is demonstrated. Some relaxations of the restrictions underlying the spring model are shown to preserve the bang-coast-bang solution.

Acknowledgements: This report describes research done at the Artificial Intelligence Laboratory of the Massachusetts Institute of Technology. Support for the laboratory's artificial intelligence research is provided in part by the Office of Naval Research under Office of Naval Research contract N00014-77-C-0389.

79 03 08 022

Though considerable effort has been expended in the study of the human motor system, the execution of even simple movements is not well understood. One current theory holds that movements are memorized in terms of final position [Bizzi et al.]. The organism selects length-tension curves of agonist and antagonist by adjusting the innervation levels so that the intersection of those curves occurs at the desired position [Feldman].

This process is illustrated by the hypothetical length-tension curves of agonist and antagonist muscles in figure 1. Suppose the system is currently at length  $L_0$  under innervation rates  $g_1$  for the agonist and  $n_1$  for the antagonist. If the innervation rate of the agonist is changed to  $g_2$ , a different agonist length-tension curve is selected and the equilibrium length shifts to  $L_1$ . Assuming no delay in tension development and ignoring velocity effects, the arrow in the figure indicates the tension course. There is an isometric buildup of tension from  $P_0$  to  $P_2$  followed by an isotonic decay to  $P_1$ , where the tension in agonist balances the tension in antagonist. The final position theory maintains that the position  $L_1$  can be reached independent of starting position merely by setting rates  $n_1$  and  $g_2$ . This theory is interesting from a manipulation viewpoint because it obviates the need for precise trajectory calculation.

There are many choices of agonist-antagonist length-tension curve pairs that have  $L_1$  as equilibrium position. One choice that could be expected to require less energy is  $n_2$  and  $g_2$ , which minimize the isometric tensions. More generally, it is conceivable that some complex sequence of innervation rates  $(n_i, g_i)$  might require less energy than a scheme which

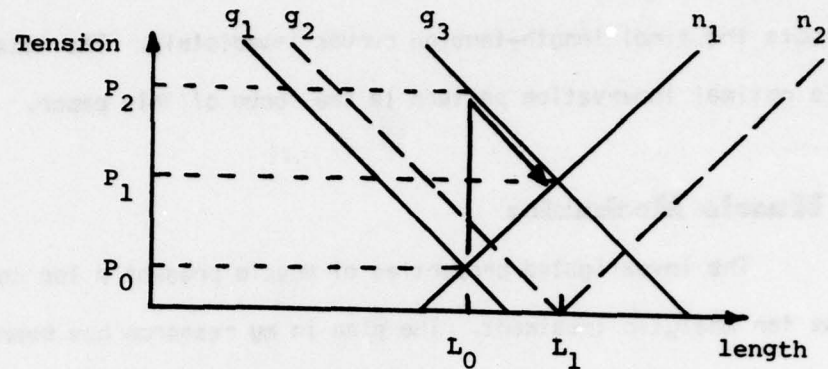


Figure 1. The equilibrium point of the intersecting length-tension curves of agonist ( $g$  labels) and antagonist ( $n$  labels) shifts from  $L_0$  to  $L_1$  when the firing rate of the agonist is raised from  $g_1$  to  $g_3$  and the antagonist rate remains at  $n_1$ .

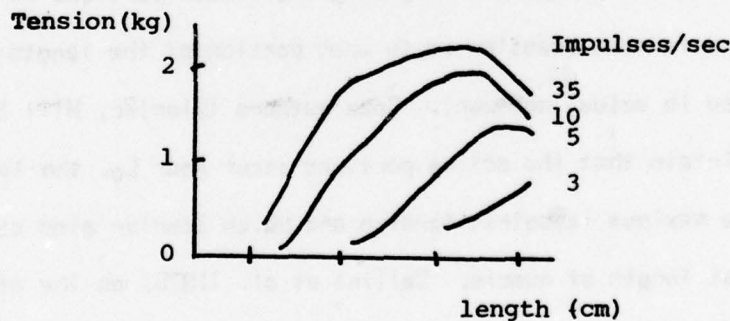


Figure 2. Length-tension curves from the cat soleus muscle (Rack and Westbury).

79 03 08 022

selects the final length-tension curves immediately. The determination of this optimal innervation pattern is the focus of this paper.

## I. Muscle Mechanics

The investigated properties of muscle present a too complicated view for analytic treatment. The plan in my research has been to simplify the muscle mechanics until an analytic solution to the optimal energy problem is possible, then to examine if the nature of the solution is changed by adding some of the excluded muscle properties. A full-blown formulation of the problem would require numerical methods for solution, and I intend eventually to carry out this analysis.

The length-tension curves in figure 1 are themselves a simplification of actual length-tension curves such as in figure 2. The simplification arises from extracting only the linear portions at short lengths. There is some question as to what portion of the length-tension curves are used in actual movement. Some authors [Zierler, Hill 1970, Cook and Stark] maintain that the active portions occur near  $L_0$ , the length at which there is maximum isometric tension and which Zierler also calls the rest or natural length of muscle. Collins et al. [1975] on the other hand report that the linear portions are used in eye movement.

For the present we accept the hypothetical length-tension curves of figure 1. The curves are also assumed parallel, as reported by Collins et al.; Rack and Westbury, however, report a decrease in slope with firing rate for this linear portion (figure 2). The curves in figure 1 lead to a model of muscle as a spring with variable zero setting. The slope  $K$  of the

curves represents the spring constant, and the variable zero setting  $L_z$  corresponds to the selection of firing rate. The force exerted by a muscle is thus  $K(L-L_z)$ .

An important simplification of muscle properties is to exclude the series elastic component. We also exclude the parallel elastic component and the active damping. The resulting muscle model is presented in figure 3. The equation of motion for the spring system of figure 3 is:

$$m \frac{d^2x}{dt^2} = -b \frac{dx}{dt} + k_s(x_s-x) - k_n(x-x_n) \quad (1)$$

Define a control variable  $U$  and a state variable  $X$  as below.

$$\dot{X} = \begin{bmatrix} x_1 \\ x_2 \end{bmatrix} = \begin{bmatrix} \dot{x} \\ \ddot{x} \end{bmatrix} \quad U = \begin{bmatrix} u_1 \\ u_2 \end{bmatrix} = \begin{bmatrix} x_s \\ x_n \end{bmatrix}$$

Setting the mass  $m = 1$ , the state variable representation of the spring system is:

$$\dot{X} = \begin{bmatrix} 0 & 1 \\ -k_s-k_n & -b \end{bmatrix} X + \begin{bmatrix} 0 & 0 \\ k_s & k_n \end{bmatrix} U \quad (2)$$

More compactly,

$$\begin{aligned} \dot{X} &= A X + B U \\ &= f(X, U, t) \end{aligned} \quad (3)$$

## II. Muscle Energetics

The energy  $E$  expended during movement equals work plus heat. The work  $W$  may be subdivided into conservative work performed on the mass  $m$  and

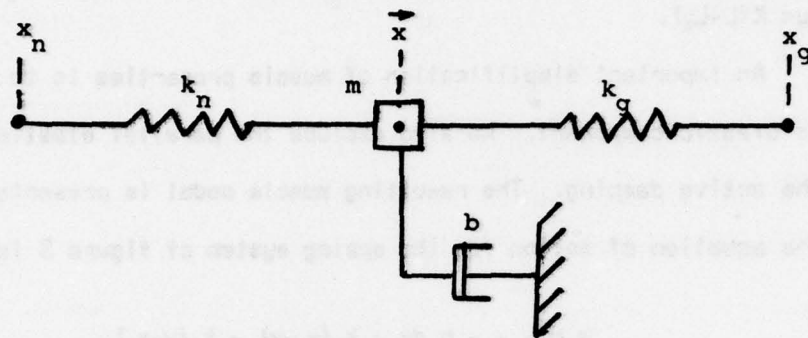


Figure 3. Simplified muscle model with equation of motion:

$$m \ddot{x} = -b \dot{x} + k_g(x_g - x) - k_n(x - x_n)$$

where

$b$  = coefficient of passive damping

$k_g$  = spring constant of the agonist

$k_n$  = spring constant of the antagonist

$m$  = mass

$x$  = position

$x_g$  = variable zero setting for the agonist

$x_n$  = variable zero setting for the antagonist

nonconservative work performed on the viscous element. The isometric heat  $Q_i$  is given off in maintaining the muscle at a particular tension  $P_0$ . The rate of energy expenditure is thus

$$\begin{aligned}\dot{E} &= P_0 v \text{ (power)} + \alpha P_0 \text{ (maintenance heat rate)} \\ &= (x_2 + a) (k_g(u_1 - x_1) + k_n(x_1 - u_2))\end{aligned}\quad (4)$$

where  $v$  is velocity and  $\alpha$  is the maintenance heat coefficient. The two force terms have been summed because each contributes to energy loss. We have excluded the shortening heat because the active damping was also excluded, and because there may be a theoretical relationship between the two [Huxley, Caplan]. The transient characteristics of heat production have also been excluded.

### III. The Euler-Lagrange Equations

The task now is to find the time varying control  $U(t)$  that minimizes the energy used in moving between two points in a fixed interval of time. Let  $V$  represent the energy consumed in applying the control  $U$  to yield the trajectory  $X$ . The problem of minimizing  $V$  is readily approached by techniques of modern control theory. The fundamental equations that the optimal control  $U(t)$  must satisfy are derived from a theorem from the calculus of variations. This theorem states that in order to find the  $n$ -vector  $X(t)$  that minimizes  $V(X)$ , where

$$V(X) = \int_{t_0}^{t_f} L(X, \dot{X}, t) dt \quad (5)$$

subject to the constraint relations

$$g_i(X, \dot{X}, t) = 0 \quad i = 1, \dots, m \leq n \quad (6)$$

then  $X(t)$  satisfies the Euler equations

$$\frac{\partial L'(X, \dot{X}, t)}{\partial x_i} - \frac{d}{dt} \frac{\partial L'(X, \dot{X}, t)}{\partial \dot{x}_i} = 0 \quad i = 1, \dots, n \quad (7)$$

where

$$L'(X, \dot{X}, t) = L(X, \dot{X}, t) + \sum_{i=1}^n \lambda_i(t) g_i(X, \dot{X}, t) \quad (8)$$

and  $\lambda_i(t)$ 's are the multiplier functions [Schultz and Meesa].

Applying this theorem to the optimal control problem, the state equations  $\dot{X} = f(X, U, t)$  represent the equality constraints.  $L$  represents the rate of change of energy  $E$ . The Hamiltonian  $H = L + \lambda^T f$  represents (8), where  $\lambda^T = [\lambda_1, \lambda_2]$ . By applying the Euler equation first for  $X$  and then for  $U$ , it can be shown that the minimizing  $U(t)$  satisfies the following two Euler-Lagrange equations [Schultz and Meesa].

$$\dot{\lambda} = -H_X \quad (9)$$

$$H_U = 0 \quad (10)$$

#### IV. The Minimum Principle

Because  $L$  is linear in the control  $U$ , there will not generally exist a minimum energy solution. To obtain a realistic solution, constraints must be placed on the control. The solution in this case will lie on the constraint boundaries [Bryson and Ho]. Constraints on  $U$ , however, make it impossible to differentiate  $H$  with respect to  $U$ .

The minimum principle of Pontryagin makes it possible to proceed from this point. Pontryagin showed that even if the control is constrained, one still obtains a minimal solution by finding the  $u^0 = u^0(X, \lambda, t)$  to minimize the Hamiltonian  $H$ , but by inspection rather than by

differentiation. After finding the minimizing  $u^0$ , one forms  $H^0 = H(X, u^0, \lambda, t)$  and then solves the following two equations [Schultz and Melso].

$$\dot{X} = \frac{\partial H^0}{\partial \lambda} \quad (11)$$

$$\dot{\lambda} = - \frac{\partial H^0}{\partial X} \quad (12)$$

There are two natural constraints that fall on the control  $U$ . First, the spring cannot push.

$$u_1 - x_1 \geq 0 \quad (13)$$

$$x_1 - u_2 \geq 0 \quad (14)$$

Second, springs have a maximum tension that they can exert. Without this constraint the solution would involve an infinite impulse. For the moment we assume the maximum tension is constant and independent of length:

$$u_1 - x_1 \leq c_1 \quad (15)$$

$$x_1 - u_2 \leq c_2 \quad (16)$$

where  $c_1$  and  $c_2$  are constants. The case of maximum tension varying with length is deferred until section XI.

## V. A Bang-Coast-Bang Solution

To facilitate inspection of the Hamiltonian, we expand  $H = \lambda^T f + L$  into three lines, the first depending on  $u_1$ , the second on  $u_2$ , and the third on neither control.

$$\begin{aligned} H = & k_g(u_1 - x_1)(a + x_2 + \lambda_2) \\ & + k_n(x_1 - u_2)(a + x_2 - \lambda_2) \\ & + x_2(\lambda_1 - b\lambda_2) \end{aligned} \quad (17)$$

To minimize  $H$  with respect to  $u_1$ , we observe that if  $a+x_2+\lambda_2 > 0$  then  $H$  is minimized when  $u_1=x_1$ . If  $a+x_2+\lambda_2 < 0$  then  $H$  is minimized with  $u_1=x_1+c_1$ . Similarly, it can be shown for  $u_2$  that when  $a+x_2-\lambda_2 < 0$  the minimizing  $u_2$  lies at  $x_1-c_2$ ; otherwise  $u_2$  is at  $x_1$ . Combining these results, one finds a bang-coast-bang solution to the minimum energy for muscle movement.

Case 1:  $\lambda_2 < -(a+x_2)$

Then  $u_1=x_1+c_1$ ,  $u_2=x_1$ .

Case 2:  $|\lambda_2| \leq (a+x_2)$

Then  $u_1=x_1$ ,  $u_2=x_1$ .

Case 3:  $\lambda_2 > (a+x_2)$

Then  $u_1=x_1$ ,  $u_2=x_1-c_2$ .

## VI. The Solution Equations

Substituting the minimizing  $u^0$  into  $H$ , one obtains three functions corresponding to the three cases.

Case 1:  $H^0 = k_1 c_1 (a+x_2+\lambda_2) + x_2 (\lambda_1 - b\lambda_2)$

Case 2:  $H^0 = x_2 (\lambda_1 - b\lambda_2)$

Case 3:  $H^0 = k_2 c_2 (a+x_2-\lambda_2) + x_2 (\lambda_1 - b\lambda_2)$

The differential equation (11) and its solution becomes for the three cases:

$$\dot{x} = \begin{bmatrix} 0 & 1 \\ 0 & -b \end{bmatrix} x + \begin{bmatrix} 0 \\ kc \end{bmatrix}$$

$$x_2(t) = x_2(t_0)e^{-b(t-t_0)} + \frac{kc}{b}(1 - e^{-b(t-t_0)}), \quad (18)$$

$$x_1(t) = x_1(t_0) + \frac{1}{b}(x_2(t_0) - x_2(t)) + \frac{kc}{b}(t-t_0) \quad (19)$$

where  $c=c_1$  and  $k=k_1$  for case 1;  $c=0$  for case 2; and  $c=-c_2$  and  $k=k_2$  for case 3. The time  $t_0$  represents the starting time. The differential equation (12) and its solution are:

$$\dot{\lambda} = \begin{bmatrix} 0 & 0 \\ 0 & 0 \\ -1 & b \end{bmatrix} \lambda - \begin{bmatrix} 0 \\ 0 \\ kc \end{bmatrix}$$

$$\lambda_1(t) = \lambda_1(t_0) \quad (20)$$

$$\lambda_2(t) = \lambda_2(t_0)e^{b(t-t_0)} + \frac{\lambda_1(t_0)+kc}{b}(1 - e^{b(t-t_0)}), \quad (21)$$

where  $c$  and  $k$  have the same meaning as above except  $c=c_2$  for case 3. Since  $\lambda_1(t)$  is constant, it appears henceforth as  $\lambda_1$  without a time dependence.

## VII. The Extremal Versus Singular Solution

It is proven in appendix A that there are exactly three events in the extremal bang-coast-bang solution: an acceleration period, a coast period, and a deceleration period. No other combination of bangs and coasts is minimizing. However, a nonextremal minimizing solution may arise from a singular arc at the switching points. The Hamiltonian (17) has the curious property that if  $\lambda_2=|\alpha+x_2|$  then the corresponding control may take on any value and still minimize  $H$ . If a control can be found to maintain  $\lambda_2=|\alpha+x_2|$  for a finite time interval, then a non-extremal solution to

energy minimization might exist. This situation is called a singular arc and arises from a performance index linear in control but quadratic in state [Bryson and Ho]. To maintain  $\lambda_2 = |a + x_2|$  for a finite time interval, all time derivatives of the two switching curves must be zero:

$$\frac{d^n(\lambda_2 + a + x_2)}{dt^n} = 0 \quad n \geq 0 \quad (22)$$

$$\frac{d^n(\lambda_2 - g - x_2)}{dt^n} = 0 \quad n \geq 0 \quad (23)$$

Carrying through the analysis for a singular arc at the first switching point (22), the time varying force during the singular arc is:

$$k_g(u_f - x_1) = \lambda_1 + ba + 3bx_2(t_1)e^{\frac{2b(t-t_1)}{2}} + \frac{3(ba+\lambda_1)(e^{\frac{2b(t-t_1)}{2}} - 1)}{2} \quad (24)$$

Unfortunately no sufficient condition has yet been developed to test whether a singular arc is minimizing, and one must compare values of the performance index for specific parameter values for the singular arc solution versus the extremal solution. Depending on the choice of  $\lambda_1$ , the force (24) takes one of the three forms in figure 4.

Of these forms only 4C has been found minimizing for some parameter combinations. To search for such combinations, a set of parameters was initially deduced from Rack and Westbury (table I). The elapsed distance  $x_f$  and the elapsed time  $t_f$  are variable and have been chosen as 0.2 cm and 0.4 sec respectively. The initial and final velocities are assumed zero. For the extremal solution (bang, coast, bang) there result 8 nonlinear equations in 8 unknowns from (18)-(21) and the initial conditions  $(x_i, t_i)$ .

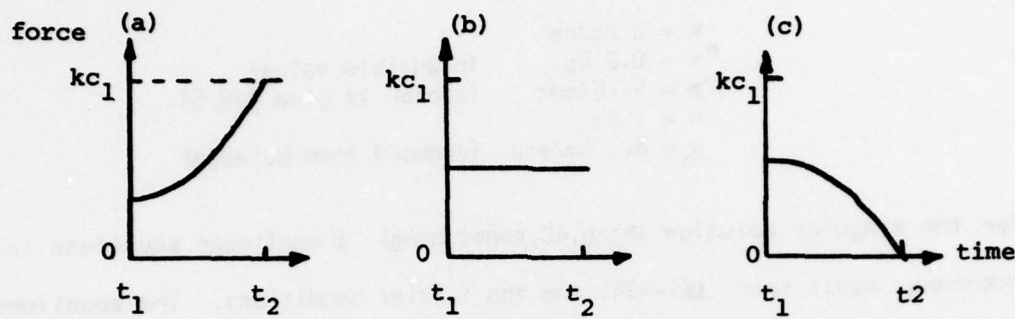


Figure 4. The three possible forms for force in a singular arc solution.

Table I

$$\begin{aligned}
 k &= 2 \text{ kg/cm} \\
 m &= 0.2 \text{ kg} \quad (\text{plausible value}) \\
 b/m &= 3.16/\text{sec} \quad (\text{chosen to give } f=0.5) \\
 c &= 1 \text{ cm} \\
 \alpha &= 0.1 \text{ cm/sec} \quad (\text{deduced from knowledge})
 \end{aligned}$$

For the singular solution (bang, 4C, coast, bang) 15 nonlinear equations in 15 unknowns result from (18)-(24) and the initial conditions. The equations were solved numerically by Newton-Raphson and gradient methods. Individual parameters were varied and energies of movement computed from (5). Solving (5), the energy for the extremal solution is

$$E = kc(\partial x_1(t_1) + \partial x_1(t_3)) + k\alpha(\partial t_1 + \partial t_3) \quad (25)$$

where  $t_1$  is the switching time from acceleration to coast,  $t_3$  is the time at the end of deceleration,  $\partial t_1$  is the duration of acceleration,  $\partial x_1(t_1)$  is the distance moved during acceleration, and  $\partial x_1(t_3)$  is the distance moved during deceleration. For the singular solution, the energy is

$$E = kc(\partial x_1(t_1) + \partial x_1(t_4)) + k\alpha(\partial t_1 + \partial t_4) + \int_{t_1}^{t_2} k_g(u_1 - x_1)(x_2(t) + \alpha) dt \quad (26)$$

where  $t_1$  is the switching time from acceleration to the singular arc 4C,  $t_2$  is the switching time from 4C to coast, and  $t_4$  is the time at the end of deceleration. The force  $k_g(u_1 - x_1)$  is given by (24), while the velocity  $x_2(t)$  is

$$x_2(t) = x_2(t_1)e^{\frac{2b(t-t_1)}{b+\lambda_1}} + \frac{bx+\lambda_1}{2b}(e^{\frac{2b(t-t_1)}{b+\lambda_1}} - 1) \quad (27)$$

The energies for the extremal versus the singular solution are compared in tables IIa-g; the units are kg cm/kg wt. In table IIc

Table IIa

<u>k</u>	<u>Singular</u>	<u>Extremal</u>
7	impossible	0.708
8	0.66117	0.66106
*10	0.6173	0.6164
28	0.5648	0.5627
38	0.5513	0.5509
48	0.54554	0.54552
58	0.5423	0.5426
100	0.536	0.537

Table IIb

<u>b</u>	<u>Singular</u>	<u>Extremal</u>
2.3	impossible	0.545
2.4	0.552036	0.552034
2.6	0.5675	0.5674
3.0	0.6020	0.6014
*10	0.6173	0.6164
4.0	0.7045	0.7038
5.0	0.820	0.824
10.0	1.45	1.51
15.0	2.13248	2.13246
15.557	impossible	2.4

Table IIc(b=k)

<u>k</u>	<u>Singular</u>	<u>Extremal</u>
7	impossible	0.664
8	0.632026	0.632023
*10	0.6173	0.6164
14	0.6442	0.6440
28	0.708	0.725

Table IID

<u>c</u>	<u>Singular</u>	<u>Extremal</u>
0.7	impossible	0.708
0.8	0.6612	0.6611
*1.0	0.6173	0.6164
2.0	0.5648	0.5627
3.0	0.5513	0.5508
4.0	0.54554	0.54551
5.0	0.5427	0.5437
6.0	0.5401	0.5407

Table IIe

<u>t<sub>1</sub></u>	<u>Singular</u>	<u>Extremal</u>
0.35	impossible	0.814
0.36	0.76123	0.76122
*0.4	0.6173	0.6164
0.45	0.512	0.511
0.5	0.444	0.445
0.6	0.358	0.369

Table IIIf(k=16, b=4)

<u>x<sub>1</sub></u>	<u>Singular</u>	<u>Extremal</u>
0.006	impossible	0.0041
0.05	0.0632	0.0634
0.1	0.1925	0.1942
*0.2	0.5647	0.5681
0.3	1.4636	1.4620
0.35	2.0120	2.0072
0.4	2.6878	2.6825
0.54	impossible	6.4598

Table IIg(k=16, b=4)

<u>a</u>	<u>Singular</u>	<u>Extremal</u>
0.05	0.6112	0.6161
*0.1	0.6647	0.6681
0.2	0.7974	0.7981
0.25	0.8633	0.8631
0.5	1.1903	1.1882
1.0	1.8393	1.8382
1.7	2.748417	2.748411
1.8	impossible	2.8784

the parameters k and b are varied simultaneously but at a fixed damping ratio of 0.5. In tables IIIf-g the parameters k and b are respectively set at 16 and 4 rather than at the table I values where the extremal solution is minimizing over the whole range of  $x_f$  and  $\alpha$ . The initial values from table I are starred in table II. A singular solution becomes minimizing with high values of k, b, c, and  $t_f$ , and with low values of  $\alpha$  and  $x_f$ . As the parameters cause the coast time to approach zero (higher b and  $x_f$ , lower k, c, and  $t_f$ ), the singular and extremal solutions become identical because the 4C portion vanishes.

For the extremal solution it is proved in appendix B that there is an upper limit on the duration of coast. It is tempting to speculate that for longer coast durations a singular solution becomes minimizing, but the singular solution in table II is not always minimizing under these conditions. Perhaps a different combination of bangs, coasts, and singular arcs would then be minimizing, but this remains an open question. Some combinations can be proved impossible, such as {bang, 4C, coast, 4A-C, bang}.

### VIII. Spring Model Relaxations: X Dependencies

A natural question is whether the minimum energy solution is changed by incorporating a more realistic muscle model. For those relaxations of the spring model involving only X dependencies, the answer is that the solution remains bang-coast-bang. The reason is that the Hamiltonian H remains linear in the control U, and the minimization of H with respect to U occurs at fixed X. Whether the solution also remains acceleration-coast-deceleration needs to be determined for each case.

Relaxations of the spring model involving X dependencies include the following.

#### 1. Position Limits on Tension

For real muscle the maximum isometric tension varies with position (figure 2). This makes  $c_1$  and  $c_2$  into functions of  $x_1$ , but the controls will still fall at the extremes wherever they are.

#### 2. Velocity Limits on Tension

Actual muscle exhibits a hyperbolic force-velocity relation. If  $P_0$  is the isometric tension, then the maximum force P that can be produced for a velocity v is [Hill 1938] (see figure 5):

$$P = P_0 - \frac{v(P_0+a)}{v+b'} \quad (28)$$

The term  $(P_0+a)/(v+b')$  can be considered the coefficient of active damping. The coefficient  $a$  has been determined as .25  $P_0$ ; the force P then becomes  $P_0 - 1.25P_0v/(v+b')$ . The literature conflicts on the value of active damping during lengthening. For consistency with the shortening heat (below), it

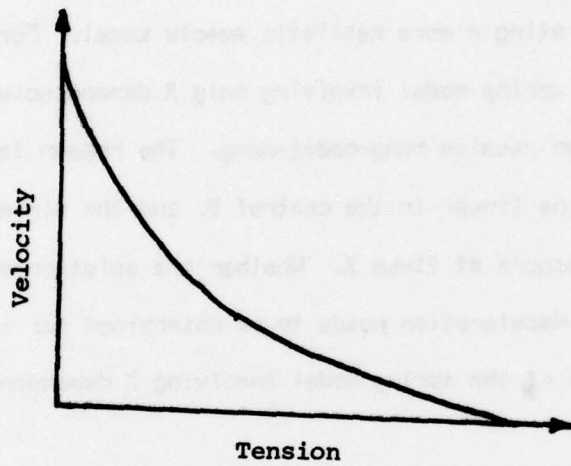


Figure 5. Tension dependence on velocity (Hill 1938).

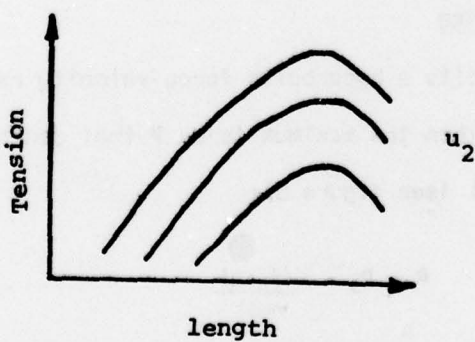


Figure 6. Hypothetical length-tension curves with the property that at any given length the slopes are the same for all choices of  $u_2$ .

is assumed the same as active damping during shortening.

Associated with the active damping is an extra heat expenditure above the isometric heat due to shortening. This shortening heat rate is (HILL 1964):

$$\dot{Q}_s = .16 P_0 v + .18 Pv \quad (29)$$

The isometric heat rate  $\dot{Q}_i$  remains  $\alpha P_0$ , but the power is now  $Pv$ .

Substituting the sum of spring forces for the isometric tension  $P_0$  and (28) for  $P$ , the energy rate is:

$$L = (k_g(u_1-x_1) + k_n(u_2-x_1))(\alpha - 0.09x_2 + \frac{1.45b'}{x_2+b'}) \quad (30)$$

Similarly it can be show that the equation of motion is:

$$\ddot{x}_2 = -b \dot{x}_2 + (1 - \frac{1.25x_2}{x_2+b'}) (k_g(u_1-x_1) - k_n(x_1-u_2)) \quad (31)$$

When these terms are combined to form the Hamiltonian, the control is seen to remain linear. Hence the solution is once again bang-coast-bang.

### 3. Spring Constant Variations with Position

One way of bringing the simplified length-tension curves of figure 1 closer to those of figure 2 is illustrated in figure 6. The spring constant  $k_n$  varies with position, but at any given position the constant  $k_n$  is the same for all controls  $u_2$ . Under these conditions the solution remains bang-coast-bang.

### 4. Parallel and Series Elastic Elements

The incorporation of these elements into the model is depicted in

figure 7. Since the parallel elastic element depends only on position, it does not change the solution. The series elastic elements and the active springs may be replaced with equivalent springs with constants  $k_s' = k_g k_e / (k_g + k_e)$  and  $k_n' = k_n k_e / (k_n + k_e)$ . This modification also has no effect on the solution.

## IX. Spring Model Relaxations: U Dependencies

In figure 2 the spring constant  $k_n$  is seen to vary with firing rate at any fixed position. The linear portions of these length-tension curves when extended seem to intersect at a common point (figure 8). In this circumstance the spring constant  $k_n$  is  $T_0 / (u_2 - x_0)$ . The  $u_2$  terms of the Hamiltonian  $H$  become:

$$\begin{aligned} H' &= \frac{T_0(x_1 - u_2)(\alpha + x_2 - \lambda_2)}{u_2 - x_0} \\ &= T_0(\alpha + x_2 - \lambda_2) \frac{(x_1 - x_0 - 1)}{u_2 - x_0} \end{aligned} \quad (32)$$

If  $\alpha + x_2 - \lambda_2 > 0$  then  $H'$  is minimized at  $u_2 = x_1$ ; otherwise  $u_2 = x_1 - c_2$ . That is to say, the solution for  $u_2$  is exactly the same as in section V. A similar analysis holds for  $u_1$ . Thus the minimizing pattern is also bang-coast-bang.

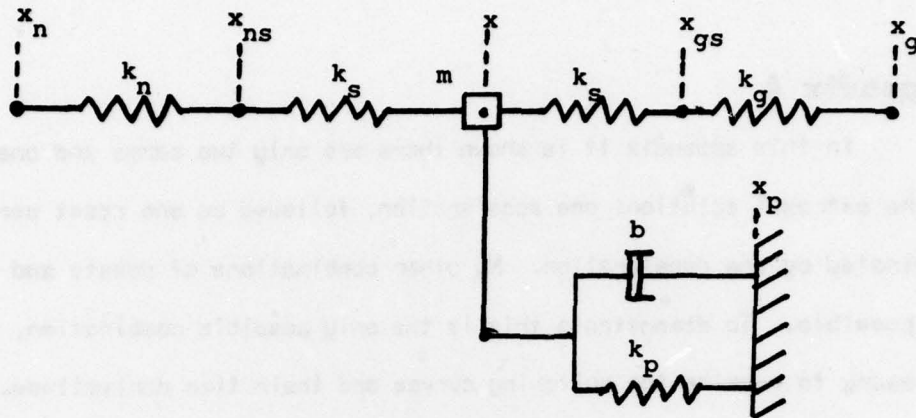


**Figure 7.** An expanded muscle model incorporating series elastic elements  $k_s$  and a parallel elastic element  $k_p$ .

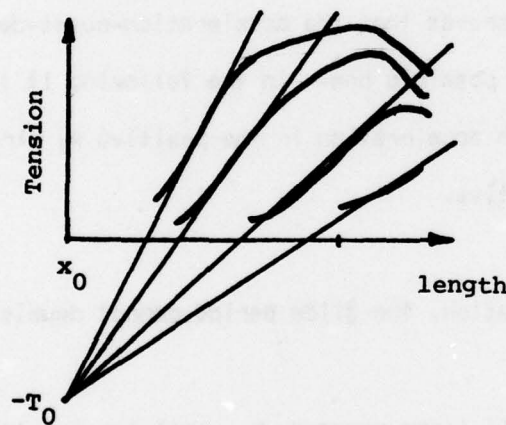


**Figure 8.** The length-tension curves of Rack and Westbury when extended meet at a point. The dependence of  $k_n$  on  $u_2$  can be characterized by  $T_0/(u_2 - x_0)$ .

## Appendix A

In this appendix it is shown there are only two bangs and one coast in the extremal solution: one acceleration, followed by one coast period, terminated by one deceleration. No other combinations of coasts and bangs are possible. To demonstrate this is the only possible combination, it is necessary to examine the switching curves and their time derivatives.

The first lemma shows that once the control has passed from acceleration to coast, then the control cannot return to another acceleration but must proceed to deceleration. The second lemma shows that once deceleration has started, the deceleration must continue until the end of the movement. This proves that the acceleration-coast-deceleration combination is the only possible one. In the following it is presumed that the movement starts with acceleration in the positive  $x_1$  direction. Hence all velocities are positive.

Lemma 1: After acceleration, the glide period cannot double back to another acceleration.

Proof: The proof of this lemma proceeds by examining the time derivative of the acceleration-coast switching curve (henceforth referred to as the slope of the switching curve). The slope of this curve is initially positive at the transition from acceleration to coast. In order for another acceleration to follow the coast period, this slope must become negative, leading to a contradiction.

At the first switching time  $t_1$ , the acceleration-coast switching curve is zero.

$$\lambda_2(t_1) + \alpha + x_2(t_1) = 0 \quad (A1)$$

After the acceleration period, the coast equations are:

$$\lambda_2(t) = \lambda_2(t_1)e^{\frac{b(t-t_1)}{b}} + \frac{\lambda_1}{b}(1 - e^{\frac{b(t-t_1)}{b}}) \quad (A2)$$

$$x_2(t) = -(\lambda_2(t_1) + \alpha)e^{-\frac{b(t-t_1)}{b}} \quad (A3)$$

Thus

$$\begin{aligned} \lambda_2(t) + \alpha + x_2(t) &= \lambda_2(t_1)e^{\frac{b(t-t_1)}{b}} + \frac{\lambda_1}{b}(1 - e^{\frac{b(t-t_1)}{b}}) \\ &\quad + \alpha - (\lambda_2(t_1) + \alpha)e^{-\frac{b(t-t_1)}{b}} \end{aligned} \quad (A4)$$

The slope of this switching curve is:

$$e^{\frac{b(t-t_1)}{b}}(b\lambda_2(t_1) - \lambda_1) + b(\lambda_2(t_1) + \alpha)e^{-\frac{b(t-t_1)}{b}} \quad (A5)$$

At  $t=t_1$ , the slope of the switching curve is:

$$2b\lambda_2(t_1) - \lambda_1 + b\alpha > 0 \quad (A6)$$

One can show this quantity cannot be less than zero. Next, suppose the coast doubles back to another acceleration. At some point the slope must go through zero. This time  $t$  is found from (A5) as:

$$e^{2b(t-t_1)} = \frac{b(\lambda_2(t_1) + \alpha)}{\lambda_1 - b\lambda_2(t_1)} > 1 \quad (A7)$$

Case 1:  $\lambda_1 - b\lambda_2(t_1) > 0$ .

Then  $\lambda_2(t_1) + \alpha > 0$ , contradicting (A1).

Case 2:  $\lambda_1 - b\lambda_2(t_1) < 0$ .

Crossmultiplying (A7) and collecting terms,

$2b\lambda_2(t_1) - \lambda_1 + b\alpha < 0$ , contradicting (A6).

Thus after acceleration, the coast period must eventually arrive at the deceleration switching point.

Lemma 2: The movement is locked in deceleration until the end.

Proof: It will be shown that if deceleration ever switches to coast, then the slope of the coast-deceleration switching curve requires an immediate return to deceleration. Hence the movement is locked in deceleration until the end.

Suppose there is a time  $t_3$  when deceleration switches to coast. At this point the coast-deceleration switching curve is zero.

$$\lambda_2(t_3) - \alpha - x_2(t_3) = 0 \quad (\text{A8})$$

The coast switching curve  $\lambda_2(t) - \alpha - x_2(t)$  is

$$\lambda_2(t_3)e^{b(t-t_3)} + \frac{\lambda_1(1-e^{-b(t-t_3)})}{b} - \alpha - x_2(t_3)e^{-b(t-t_3)} \quad (\text{A9})$$

The slope of (A9) is:

$$e^{b(t-t_3)} (b\lambda_2(t_3) - \lambda_1) + bx_2(t_3)e^{-b(t-t_3)} \quad (\text{A10})$$

At time  $t_3$  the slope (A10) is  $b\lambda_2(t_3) - \lambda_1 + bx_2(t_3)$ . This is positive since  $\lambda_2(t_3) > 0$ ,  $x_2(t_3) > 0$ , and  $\lambda_1 < 0$  (Lemma 3). This means that deceleration would bounce off the coast boundary and immediately continue the deceleration. Furthermore, since the slope is positive, the deceleration would not immediately switch back to coasting, causing chattering.

Lemma 3:  $\lambda_1 < 0$ .

Proof: At the second switching point  $t_2$  we have

$$\lambda_2(t_2) - \alpha - x_2(t_2) = 0 \quad (\text{A11})$$

From (A2) and (A3), this becomes

$$\frac{\lambda_2(t_1)e^{b(t_2-t_1)}}{b} + \frac{\lambda_1(1-e^{-b(t_2-t_1)})}{b} - \alpha + (\lambda_2(t_1) + \alpha)e^{-b(t_2-t_1)} = 0 \quad (\text{A12})$$

Rearranging,

$$\frac{\lambda_1(1-e^{-b(t_2-t_1)})}{b} = -\lambda_2(t_1)(e^{b(t_2-t_1)} + e^{-b(t_2-t_1)}) + \alpha(1-e^{-b(t_2-t_1)}) \quad (\text{A13})$$

From (A1) and (A3) we find an expression for  $\lambda_2(t)$ .

$$\lambda_2(t_1) = -\alpha - \frac{k_2 c_1 (1-e^{-b(t_1-t_0)})}{b} \quad (\text{A14})$$

Substituting into (A13),

$$\begin{aligned} \frac{\lambda_1(1-e^{-b(t_2-t_1)})}{b} &= \frac{k_2 c_1 (1-e^{-b(t_1-t_0)})}{b} (e^{b(t_2-t_1)} + e^{-b(t_2-t_1)}) \\ &\quad + \alpha(1+e^{-b(t_2-t_1)}) \end{aligned} \quad (\text{A15})$$

Thus

$$\lambda_1 = \frac{k_2 c_1 (1-e^{-b(t_1-t_0)}) (e^{b(t_2-t_1)} + e^{-b(t_2-t_1)}) + \alpha(1+e^{-b(t_2-t_1)})}{1-e^{-b(t_2-t_1)}} \quad (\text{A16})$$

Since the numerator is positive and the denominator is negative,  $\lambda_1$  is negative.

Taken together, these lemmas show that acceleration passes through coast to deceleration. There is no possible variation in this scheme. It is also possible to show the movement cannot start by coasting followed by acceleration.

## Appendix B

A surprising limitation on the value of  $t_2 - t_1$ , the duration of the coasting time, has been found. The switching curve during acceleration is:

$$\lambda_2(t) + \alpha + x_2(t) = \lambda_2(t_0) e^{b(t-t_0)} + \frac{\lambda_1 + k_g c_1}{b} (1 - e^{-b(t-t_0)}) + \alpha + \frac{k_g c_1}{b} (1 - e^{-b(t-t_0)}) \quad (B1)$$

The slope of this switching curve is:

$$e^{b(t-t_0)} (b\lambda_2(t_0) - \lambda_1 - k_g c_1) + k_g c_1 e^{-b(t-t_0)} \quad (B2)$$

At the first switching time  $t_1$ , the switching function (B1) is zero.

Rearranging (B1) for  $t=t_1$ ,

$$e^{b(t_1-t_0)} (\lambda_2(t_0) - \frac{\lambda_1 + k_g c_1}{b}) = - \frac{\lambda_1 + k_g c_1}{b} - \alpha - \frac{k_g c_1}{b} (1 - e^{-b(t_1-t_0)}) \quad (B3)$$

Substituting (B3) into (B2), the slope at  $t_1$  is:

$$- 2k_g c_1 (1 - e^{-b(t_1-t_0)}) - \lambda_1 - b\alpha \quad (B4)$$

Substituting for  $\lambda_1$  from (A16),

$$\frac{k_g c_1 (1 - e^{-b(t_1-t_0)}) (2 + e^{-b(t_2-t_1)} - e^{-b(t_2-t_1)}) + 2b\alpha}{e^{b(t_2-t_1)} - 1} \quad (B5)$$

Since  $\text{slope}(t_1) \geq 0$  and since the denominator is positive, so is the numerator.

$$k_g c_1 (1 - e^{-b(t_1-t_0)}) (2 + e^{-b(t_2-t_1)} - e^{-b(t_2-t_1)}) + 2b\alpha \geq 0 \quad (B6)$$

Because  $2 + e^{-b(t_2-t_1)} - e^{b(t_2-t_1)}$  is a decreasing function of  $t_2$ , at some point (B6) becomes zero. Solving then for  $e^{b(t_2-t_1)}$ ,

$$\frac{bg + \sqrt{(bg+k_g c_1(1-e^{-b(t_1-t_0)}))^2 + (k_g c_1(1-e^{-b(t_1-t_0)}))^2}}{k_g c_1(1-e^{-b(t_1-t_0)})} + 1 \quad (B7)$$

As  $t_2$  increases,  $t_1$  will decrease. However,  $t_1$  does not decrease enough to offset the effect of the  $t_2$  increase. If  $a=0$ , (B7) reduces to

$$e^{b(t_2-t_1)} = 1 + \sqrt{2} \quad (B7a)$$

Strangely, in this circumstance  $t_2-t_1$  depends only on  $b$ .

## References

1. Bizzì, Emilio, Andres Polit, and Pietro Morasso [1976]: Mechanisms underlying achievement of final head position. J. Neurophys., 39:435-444.
2. Bryson, A.E. and Yu-Chi Ho [1969]: Applied Optimal Control. Ginn and Company, Waltham, Mass.
3. Caplan, S.R. [1966]: A characteristic of self-regulated linear energy converters. The Hill force-velocity relation for muscle. J. Theor. Biol., 11:63.
4. Collins, Carter C., David O'Meara and Alan B. Scott [1975]: Muscle tension during unrestrained eye movements. J. Physiol., 245:351-369.
5. Cook, G. and L. Stark [1967]: Derivation of a model for the human eye positioning mechanism. B. Math. Biophys. 29:153-174.
6. Feldman, A.G. [1974a]: Change of muscle length due to shift of the equilibrium point of the muscle-load system. Biofizika 19:534-538.
7. Feldman, A.G. [1974b]: Control of muscle length. Biofizika 19:749-753.
8. Hill, A.V. [1938]: The heat of shortening and the dynamic constants of muscle. Proc. R. Soc. Lond. (Biol.), 126:136.
9. Hill, A.V. [1964]: The effect of load on the heat of shortening of muscle. Proc. R. Soc. Lond. (Biol.), 159:297.
10. Hill, A.V. [1970]: First and Last Experiments in Muscle Mechanics. Cambridge University Press, London.
11. Huxley, A.F. [1957]: Muscle structure and theories of contraction. Prog. Biophys. Chem., 7:255.
12. Rack, P.M.H. and D.R. Westbury [1969]: The effects of length and stimulus rate on tension in the isometric cat soleus muscle. J. Physiol., 204:443-460.
13. Schultz, D.G. and James L. Meiss [1967]: State Functions and Linear Control Systems. McGraw-Hill.
14. Woledge, R.C. [1971]: Heat production and chemical change in muscle. In: Progr. Biophys. Mol. Biol., 22:37.
15. Zierler, K.L. [1974]: Mechanism of muscle contraction and its energetics. In: Medical Physiology, V.B. Mountcastle, ed., 1:636-650.